International Journal of Electrical and Computer Engineering (IJECE)
Vol. 10, No. 4, August 2020, pp. 4109~4117
ISSN: 2088-8708, DOI: 10.11591/ijece.v10i4.pp4109-4117

Computational scrutiny of image denoising method found on DBAMF under SPN surrounding

Vorapoj Patanavijit
Department of Electrical and Electronic Engineering, Faculty of Engineering,
Assumption University of Thailand, Thailand

Article Info

Article history:

Received Sep 3, 2019
Revised Feb 27, 2020
Accepted Mar 8, 2020

Keywords:

AMF (adaptive median filter)
Digital image denoising
ROAD (rank-ordered absolute differences)
SMF (standard median filter)

ABSTRACT

Traditionally, rank order absolute difference (ROAD) has a great similarity capacity for identifying whether the pixel is SPN or noiseless because statistical characteristic of ROAD is desired for a noise identifying objective. As a result, the decision based adaptive median filter (DBAMF) that is found on ROAD technique has been initially proposed for eliminating an impulsive noise since 2010. Consequently, this analyzed report focuses to examine the similarity capacity of denoising method found on DBAMF for diverse SPN Surrounding. In order to examine the denoising capacity and its obstruction of the denoising method found on DBAMF, the four original digital images, comprised of Airplane, Pepper, Girl and Lena, are examined in these computational simulations for SPN surrounding by initially contaminating the SPN with diverse intensity. Later, all contaminated digital images are denoised by the denoising method found on DBAMF. In addition, the proposed denoised image, which is computed by this DBAMF denoising method, is confronted with the other denoised images, which is computed by standard median filter (SMF), gaussian filter and adaptive median filter (AMF) for demonstrating the DBAMF capacity under subjective measurement aspect.

Corresponding Author:

Vorapoj Patanavijit,
Department of Electrical and Electronic Engineering,
Faculty of Engineering, Assumption University,
PKE Bldg., 2nd Flr., 88 Moo 8 Bang Na-Trad Km. 26, Bangsaothong, Samuthprakarn 10540, Thailand.
Email: patanavijit@yahoo.com

1. RELEVANT RESEARCHED OF DENOISING METHODS FOF SPN

Because of diverse reasons such as fault in synchronization of analog to digital process, malfunction of CCD chip, fault in addressing of storage process, and fault in transmission, etc., the impulsive noise [1-5] can be separated into two main categories: Salt and pepper noise (SPN) and random magnitude impulsive noise (RMIN) from algebraic formulation aspect. Hence, may SPN denoising methods [1-9] have been examined for more than two decades due to demanding of modern digital image applications [10-23]: retina classification, super resolution, emotion classification, etc. At first, the SMF (Standard Median Filter) [8, 24] is discovered in 1975 for excluding SPN (Salt and Pepper Noise) and, later, is become one of the most capable and practical denoising methods from the fact that this method is low computation and high capability. The denoised method based on Gaussain filter [24] is desired for well applying on Gaussain noise but this method has poor performance for SPN. Later, adaptive median filter (AMF) [7, 25], which is improved from the SMF denoising method by varing its window size, is proposed and its performance is better than the SMF denoising method. After two decades, the modern decision based adaptive median filter (DBAMF) [3, 25], which is improved from the SMF-denoising method, is discovered for denoising RMIN in 2010.

The DBAMF method is formulated from two main schemes: noise classification schemes (that is found on ROAD (Rank Order Absolute Difference)) and noise exclusion schemes (that is found on SMF [5, 25]). Unfortunately, there are no securitized researches of DBAMF capability and its constraint when this denoising

method is implemented on SPN at diverse intensity. Consequently, this analyzed report focuses to examine the similarity capacity of denoising method found on DBAMF [3] for diverse SPN surrounding in order to analytically understand its upper bound of its performance and its limitation for future implementations.

2. THE PRIMARY CONCEPT OF DBAMF

The distorted portrait is mathematically explained as $\mathbf{Y}$ and the portrait intensity is mathematically explained as $y(i,j)$. The DBAMF scheme [3, 25] can be separated into two primary schemes: noise recognizing scheme and noise repairing scheme, which can be comprehensively reviewed as upcoming.

2.1. The primary concept of noise recognizing scheme

The performing arithmetic concept of the noise recognizing scheme can be reviewed as.

- Determine the calculated square region $\underline{\mathbf{W}}_{3\times3}$ at 3×3 ($w=3$) of the processed portrait pixels at (i,j) coordination.
- Determine the absolute difference ($D_{s,t}(y_{i,j})$) with normalization, so called NAD, of the processed portrait pixel with middlemost coordination (i,j), which can be comprehensively clarified as upcoming.

$$D_{s,t}(y_{i,j}) = \left| y_{i,j} - y_{s,t} \right| / 255 \tag{1}$$

- Determine the vector of absolute difference ($D_{s,t}(y_{i,j})$) with normalization, so called NROAD (the processed portrait pixel with middlemost coordination (i,j)), which are aligned for storing only five undermost values from eigh values in the calculated square region. Later, the statistical mean of NROAD can be comprehensively clarified as upcoming.

$$\text{ROAD}_{m=5} = \tfrac{1}{5}\sum_{m=1}^{5} D_{s,t}(y_{i,j}) \tag{2}$$

- From NROAD, if the statistical mean of NROAD, which fluctuates between 0.00 to 1.00 for all pixels in the processed portrait, is greater than a stable constant T_0 [3, 25] then the processed portrait pixel is recognized as the distorted pixel, otherwise then the processed portrait pixel is recognized as the noise-free pixel. Therefore, the the Noise Detected Matrix can be comprehensively clarified as upcoming.

$$\text{NDM} = 1, \text{if } \text{ROAD}_{m=5} \geq T_0 \text{ otherwise } 0, \text{if } \text{ROAD}_{m=5} < T \tag{3}$$

From the above noise recognizing scheme of the DBAMF, we can comprehensively display this processing scheme in the upcoming flowchart as Figure 1.

2.2. The primary concept of noise repairing scheme

The performing arithmetic concept of the noise repairing scheme can be reviewed as.

- Determine the calculated square region $\underline{\mathbf{W}}_{3\times3}$ at 3×3 ($w=3$) of NDM (noise detected matrix) at (i,j) coordination.
- From the calculated square region of NDM, if the total noise-free pixels is fewer than three pixels then the dimension of the calculated square region $\underline{\mathbf{W}}_{3\times3}$ is expanded by one and the Step 2 is reexecuted.
- From the calculated square region of NDM, if the total distorted pixels is more than two pixels then the repaired pixel is executed by as upcoming.

$$\hat{Y}_{i,j} = \text{median}\left\{ Y_{i-s,j-t} \middle| (s,t) \in W_F \right\} \tag{4}$$

- The duplicated sheme is re executed for every pixels in the processed portrait pixels.

From the above noise repairing scheme of the DBAMF, we can comprehensively display this processing scheme in the upcoming flowchart as Figure 2.

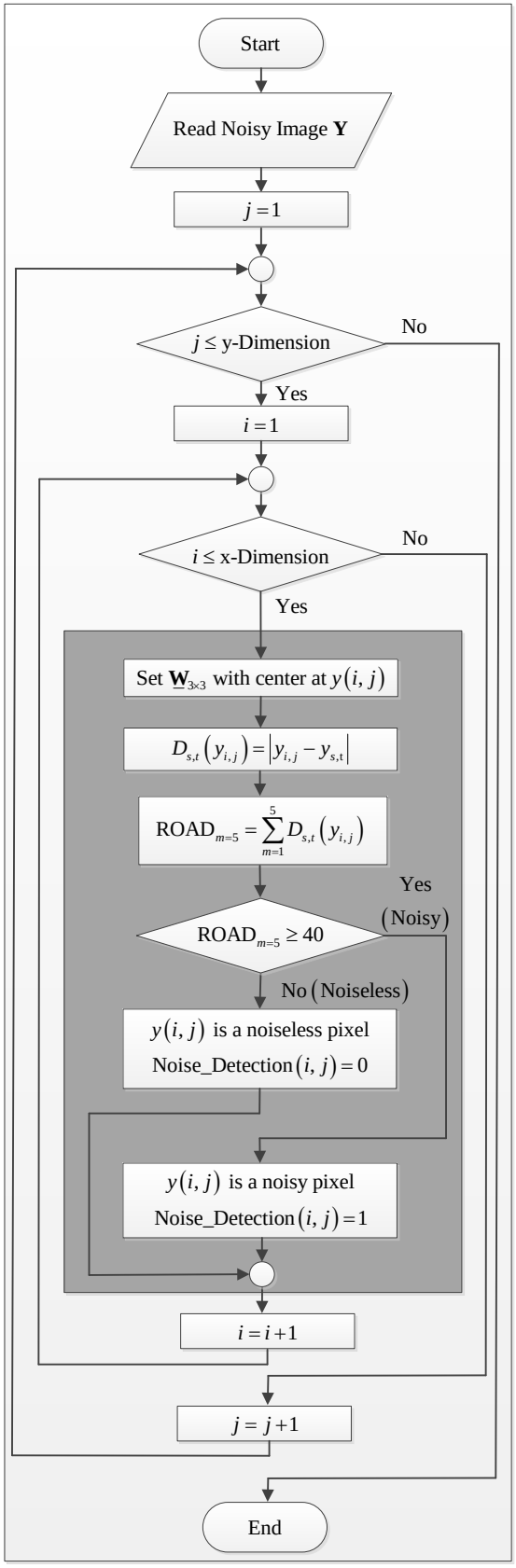

Figure 1. The arithmetic concept of the noise recognizing scheme

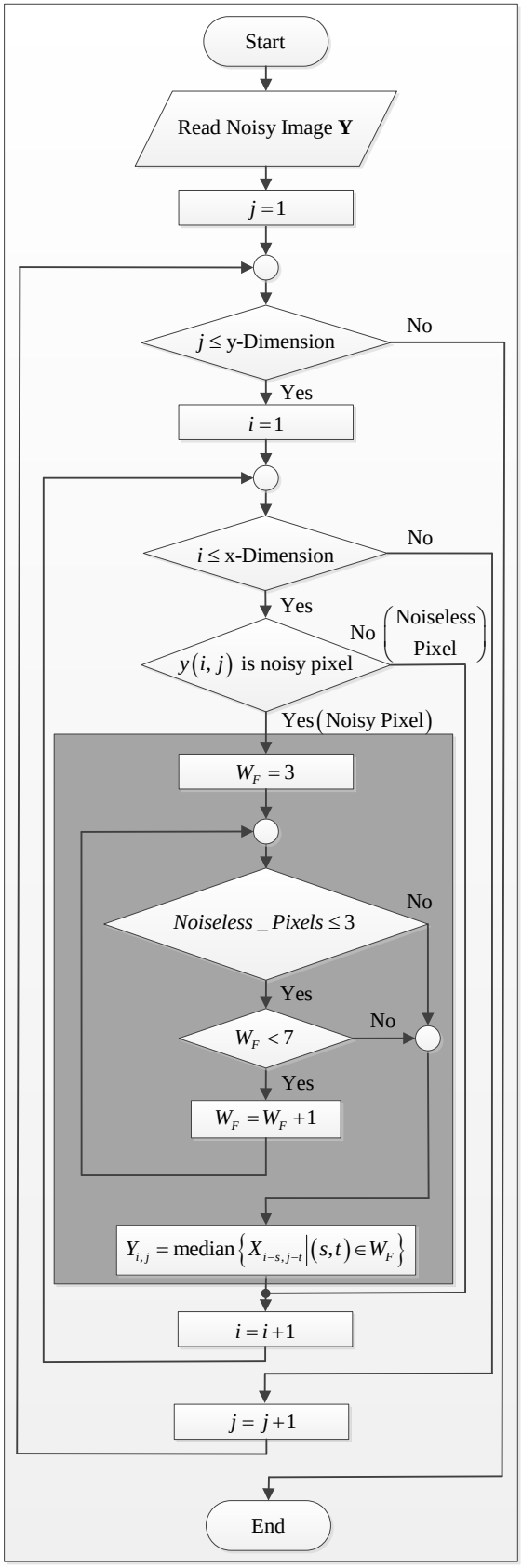

Figure 2. The arithmetic concept of the noise repairing scheme

3. THE COMPUTATIONAL EXAPLE OF DBAMF CONCEPT

In first cases, this part comprehensively reviewes the calculation of the example of DBAMF noise recognizing scheme as in Figure 3(a) for obviously reviewing the processed calculation where $y_{i,j}$ is a distored pixel, which is distorted by for salt and pepper noise ($y_{i,j}=255$). Later, the distored pixel is repaired as in Figure 3(b) where the distored pixel ($y_{i,j}=255$) is repaired to be the repaired pixel ($y_{i,j}=118$).

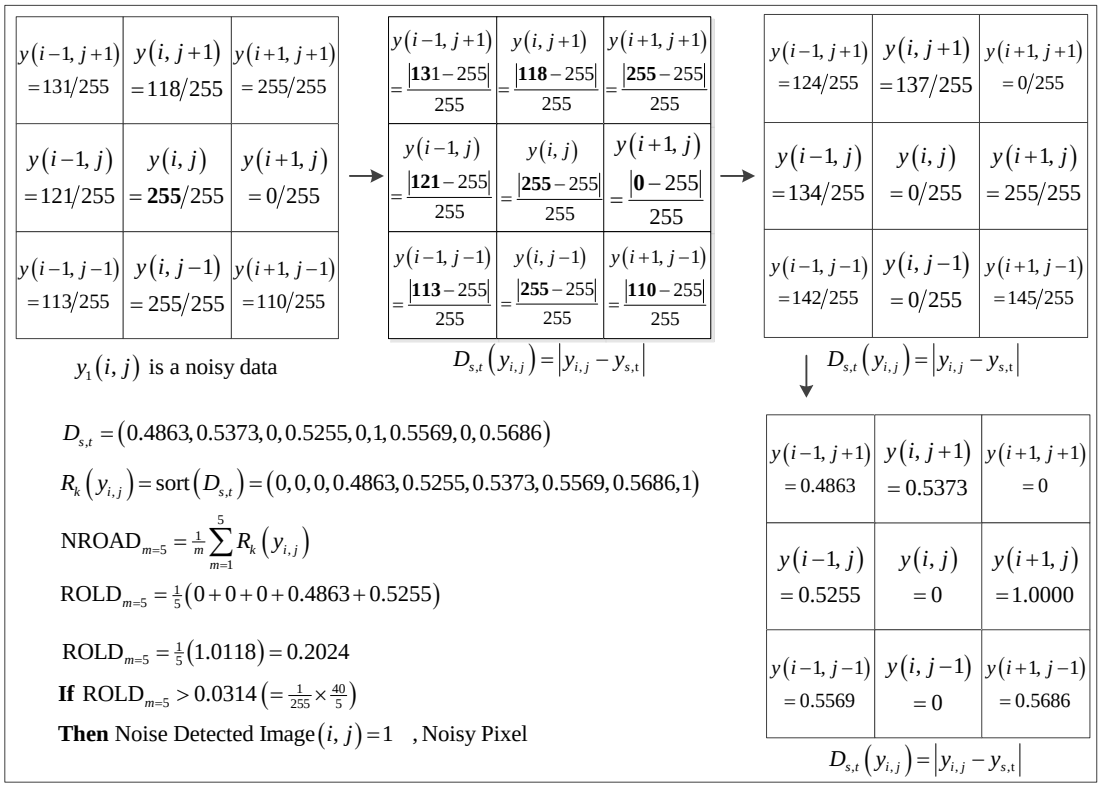

(a)

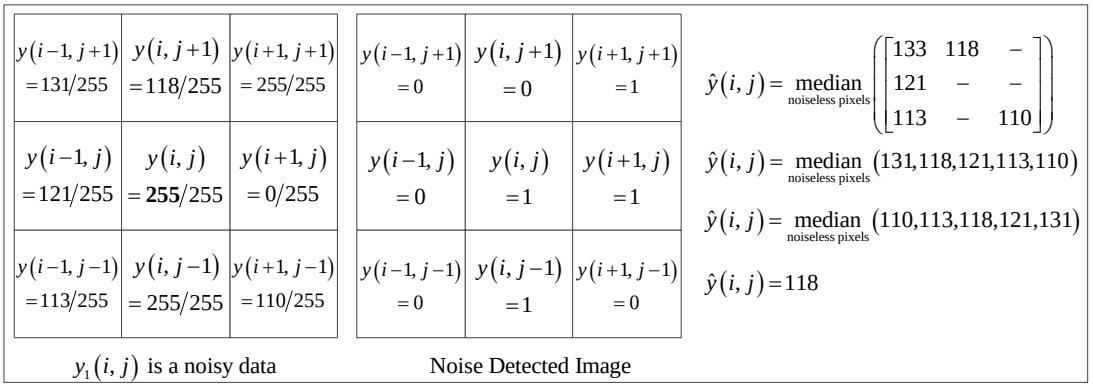

Figure 3 (a). The computer example of the noise recognizing scheme,
(b) The computer example of the noise repairing scheme

4. RESULTS AND DISCUSSION

In this examining of the DBAMF denoising capacity, the calculation software in this analyzed report is MATLAB program that is run on workstation computers with the hardware detail: the CPU is Intel i7-6700HQ and the internal memory is 16 GB and all workstation computers simulate on diverse portraits,

which are contained of Airplane, Pepper, Girl and Lena, at numerous SPN densities where all diverse portraits that are distorted by adding synthesized SP noise. All distorted portraits are repaired for obtaining the finest quality and best PSNR by executing the image denoising method found on DBAMF for first noise recognizing scheme (in order to recognize whether the pixel is noise-free or noisy) and, later, noise repair scheme (in order to repair only the noisy pixels).

4.1. The experimental investigation of noise recognizing scheme

This simulated experiment section investigates the optimized stable constant T_0 for providing the finest quality and best PSNR as shown in Table 1-4. The stable constant T_0, which fluctuates between 0.00 to 1.00 for all pixels in the processed portrait, ultimately impacts to the denoising capacity of DBAMF method. Consequently, this computer examining comprehensively determines the stable constant T_0, which make the finest quality and best PSNR when each distorted portrait is executed by denoising capacity of DBAMF method. The numerous digital portraits (which are contained of Airplane, Pepper, Girl and Lena) are used to analyze the stable constant T_0 by varying from 0.00 to 0.50 at 0.025 incremented steps as displayed in Table 1 to Table 4, respectively.

- From these computer examining of Girl in Table 1, the optimized pre-specified constant T_0 is about 0.1153± 0.0005 or be fluctuated from 0.075 to 0.150 for making the finest DBAMF denoising capacity
- From these computer examining of Pepper in Table 2, the optimized pre-specified constant T_0 is about 0.1069±0.0010 or be fluctuated from 0.025 to 0.150 for making the finest DBAMF denoising capacity.

Table 1. The denoising capacity interconnection of PSNR and the stable constant T_0 for airplane image

Fix	PSNR (dB)																	
Con	5	10	15	20	25	30	35	40	45	50	55	60	65	70	75	80	85	90
0.025	25.66	25.46	24.34	23.47	22.36	21.13	19.17	18.16	16.42	15.01	12.96	11.75	7.50	6.74	5.88	5.06	4.77	4.79
0.050	28.99	27.72	26.79	25.19	23.94	21.99	20.29	18.41	**17.04**	15.32	13.70	12.01	10.42	8.71	6.82	5.93	5.78	5.25
0.075	31.85	29.96	27.88	**26.22**	**25.01**	**22.18**	**20.52**	**18.59**	16.92	**15.43**	**13.92**	12.12	10.71	8.96	7.93	6.57	6.11	5.25
0.100	33.47	31.15	28.41	25.90	24.80	21.97	20.31	18.38	16.67	15.41	13.81	**12.33**	10.81	9.49	8.30	7.59	6.70	6.01
0.125	**36.50**	**31.54**	**29.92**	25.15	24.09	21.98	20.05	18.12	16.43	15.09	13.72	12.29	10.92	9.75	8.56	7.85	6.81	6.31
0.150	36.24	31.01	28.06	25.04	22.80	21.06	19.22	17.45	15.90	14.64	13.26	12.02	**10.94**	**9.84**	8.65	**7.99**	**7.00**	**6.33**
0.175	34.35	29.40	26.92	24.04	22.34	19.68	18.41	16.78	15.34	14.09	12.92	11.56	10.69	9.51	**8.68**	7.63	6.84	6.32
0.200	32.26	28.01	25.44	22.69	20.84	18.48	17.01	15.53	13.94	12.97	11.90	10.78	9.84	8.91	8.01	7.35	6.69	6.09
0.225	32.22	27.05	24.57	21.69	19.83	17.70	16.02	14.35	12.94	11.87	10.82	9.77	8.67	8.15	7.24	6.67	6.10	5.60
0.250	30.58	26.59	24.06	21.35	19.54	17.52	15.93	14.25	12.91	11.83	10.81	9.38	8.67	8.16	6.97	6.72	5.90	5.18
0.275	29.93	26.08	23.60	20.93	19.19	17.26	15.68	14.16	12.78	11.66	10.70	9.63	8.47	8.05	7.09	6.90	5.93	5.58
0.300	29.46	25.58	23.12	20.49	18.77	16.88	15.34	13.89	12.57	11.54	10.58	9.59	8.70	8.21	7.19	6.87	5.87	5.35
0.325	29.00	25.04	22.55	20.05	18.35	16.52	15.02	13.62	12.38	11.36	10.38	9.43	8.65	8.01	7.20	6.72	6.07	5.62
0.350	28.56	24.55	22.05	19.63	17.98	16.20	14.76	13.40	12.17	11.17	10.26	9.37	8.64	8.00	7.23	6.77	6.02	5.69
0.375	28.07	24.08	21.53	19.15	17.54	15.80	14.43	13.14	11.94	10.97	10.09	9.26	8.48	7.93	7.20	6.71	6.06	5.71
0.400	27.37	23.29	20.48	18.04	16.48	14.87	13.49	12.29	11.14	10.27	9.54	8.78	8.10	7.61	6.97	6.54	6.03	5.66
0.425	26.95	22.49	19.43	17.12	15.37	13.77	12.50	11.40	10.31	9.52	8.85	8.16	7.57	7.17	6.63	6.29	5.85	5.56
0.450	26.67	22.17	19.13	16.81	15.12	13.57	12.30	11.21	10.18	9.39	8.74	8.06	7.48	6.99	6.55	6.19	5.77	5.48
0.475	26.32	21.84	18.88	16.59	14.94	13.40	12.19	11.12	10.10	9.33	8.69	8.01	7.43	6.93	6.48	6.10	5.67	5.37
0.500	25.96	21.61	18.63	16.40	14.78	13.25	12.08	11.03	10.03	9.29	8.65	8.00	7.43	6.95	6.50	6.12	5.71	5.40

Table 2. The denoising capacity interconnection of PSNR and the stable constant T_0 for pepper image

Fix	PSNR (dB)																	
Con	5	10	15	20	25	30	35	40	45	50	55	60	65	70	75	80	85	90
0.025	25.63	24.29	23.60	21.79	20.88	20.19	19.01	17.59	16.31	14.75	12.92	10.69	8.55	6.59	6.36	5.82	5.91	5.58
0.050	29.43	27.77	25.96	24.17	22.85	20.99	20.03	18.22	16.82	**15.33**	13.43	11.52	9.29	7.02	6.26	5.84	5.77	5.63
0.075	32.75	29.73	27.61	24.45	23.31	**21.76**	**20.35**	**18.40**	**17.10**	15.20	**13.58**	11.94	9.46	8.05	7.09	6.69	6.16	5.78
0.100	35.44	31.91	**28.58**	**25.91**	**23.67**	21.66	20.17	18.17	16.84	15.03	13.34	**11.95**	**10.35**	8.35	7.34	6.45	6.43	5.92
0.125	37.08	31.50	27.08	25.81	23.06	21.26	19.42	17.53	16.09	14.59	13.04	11.78	10.32	8.80	7.53	**7.04**	**6.51**	6.09
0.150	**37.60**	**32.86**	26.92	25.27	21.71	20.48	18.60	16.78	15.37	13.85	12.68	11.18	10.02	**8.90**	**7.84**	6.97	6.47	**6.21**
0.175	36.56	31.53	26.24	24.13	20.85	19.50	17.63	16.05	14.75	13.22	12.13	10.60	9.76	8.54	7.79	6.74	6.43	6.19
0.200	35.36	29.79	25.21	23.10	20.26	18.52	16.63	15.08	13.87	12.42	11.49	10.09	8.96	8.04	7.17	6.35	6.18	5.78
0.225	33.49	28.50	25.04	22.23	19.47	17.80	16.08	14.54	13.39	11.89	11.01	9.92	8.95	8.07	7.21	6.52	6.04	5.97
0.250	32.13	27.37	24.09	21.36	18.87	17.22	15.71	14.19	12.99	11.72	10.65	9.58	9.14	7.94	7.30	6.66	6.09	5.73
0.275	30.93	26.20	23.13	20.36	18.16	16.67	15.12	13.66	12.57	11.26	10.50	9.57	8.69	7.86	7.47	6.70	6.18	5.82
0.300	29.67	25.16	22.36	19.72	17.63	16.14	14.60	13.24	12.25	11.07	10.22	9.36	8.50	7.80	7.37	6.63	6.19	5.88
0.325	28.69	24.26	21.52	18.99	17.02	15.63	14.16	12.87	11.87	10.84	10.04	3.38	8.47	7.79	7.38	6.66	6.34	5.94
0.350	27.75	23.29	20.58	18.19	16.48	14.97	13.65	12.45	11.50	10.54	9.78	9.17	8.34	7.72	7.35	6.72	6.38	5.97
0.375	26.90	22.52	19.68	17.50	15.81	14.40	13.15	12.04	11.11	10.21	9.51	8.80	8.20	7.61	7.14	6.72	6.33	5.99
0.400	26.05	21.63	18.85	16.71	15.07	13.72	12.52	11.49	10.61	9.79	9.13	8.50	7.94	7.42	6.98	6.62	6.27	5.96
0.425	25.07	20.91	18.23	16.20	14.60	13.28	12.18	11.19	10.33	9.56	8.94	8.33	7.81	7.32	6.90	6.56	6.22	5.92
0.450	24.24	20.29	17.72	15.82	14.27	13.02	11.97	11.01	10.18	9.44	8.84	8.25	7.75	7.27	6.85	6.51	6.16	5.85
0.475	23.60	19.77	17.28	15.48	13.98	12.81	11.78	10.88	10.07	9.36	8.77	8.20	7.72	7.25	6.84	6.50	6.15	5.85
0.500	23.09	19.28	16.90	15.17	13.73	12.59	11.60	10.73	9.96	9.29	8.72	8.17	7.71	7.25	6.86	6.53	6.20	5.89

- From these computer examining of Lena in Table 3, the optimized pre-specified constant T_0 is about 0.1125±0.0042 or be fluctuated from 0.050 to 0.175 for making the finest DBAMF denoising capacity.
- From these computer examining of Airplane in Table 4, the optimized pre-specified constant T_0 is about 0.1097±0.0014 or be fluctuated from 0.050 to 0.150 for making the finest DBAMF denoising capacity.

Table 3. The denoising capacity interconnection of PSNR and the stable constant T_0 for girl image

Fix	PSNR (dB)																	
Con	5	10	15	20	25	30	35	40	45	50	55	60	65	70	75	80	85	90
0.025	27.01	26.00	25.23	24.60	23.68	21.44	19.68	18.01	16.49	14.86	13.41	11.80	10.35	8.74	7.41	7.04	5.59	4.82
0.050	32.19	30.68	29.24	26.97	25.24	23.03	20.30	18.47	16.82	15.13	13.59	12.13	10.43	9.20	7.78	7.27	5.83	5.05
0.075	34.88	33.50	30.65	27.60	25.81	**23.26**	**20.60**	18.37	16.81	15.11	13.61	12.11	10.85	9.44	8.43	7.02	6.28	5.24
0.100	37.65	34.48	31.36	27.55	**26.07**	22.88	20.28	18.40	**16.93**	15.06	13.68	**12.29**	**10.94**	9.51	8.64	7.30	**6.52**	**5.29**
0.125	39.12	**35.94**	**32.09**	**29.40**	25.98	23.19	19.87	**18.49**	16.72	**15.16**	**13.69**	12.26	10.85	**9.56**	8.70	7.40	6.49	5.04
0.150	**39.20**	34.97	31.87	28.81	25.51	22.18	20.47	18.15	16.65	15.00	13.66	12.26	10.90	9.53	**8.75**	**7.50**	6.39	5.15
0.175	38.79	34.58	31.53	28.11	25.10	21.76	19.94	17.80	16.43	14.73	13.43	11.95	10.84	9.42	8.61	7.43	6.31	5.27
0.200	38.14	33.58	30.03	26.66	24.06	20.80	19.27	17.09	15.62	14.09	12.84	11.61	10.52	8.93	8.56	7.24	6.16	5.07
0.225	36.72	32.00	28.66	25.52	23.05	20.12	18.50	16.27	15.05	13.59	12.37	11.19	10.11	8.94	8.42	6.93	6.04	4.96
0.250	35.60	30.98	26.73	23.08	19.81	17.92	15.53	13.72	12.56	11.00	9.97	8.68	8.07	7.18	6.38	5.65	5.13	4.52
0.275	34.43	30.14	26.37	22.88	19.72	17.87	15.51	13.79	12.50	10.98	9.98	9.12	7.96	7.31	6.65	5.66	5.04	4.86
0.300	33.21	29.34	25.96	22.63	19.58	17.79	15.48	13.75	12.49	10.98	9.98	9.13	7.98	7.31	6.66	5.75	5.08	4.89
0.325	33.01	29.18	25.84	22.55	19.53	17.76	15.45	13.74	12.47	10.98	9.97	9.13	8.00	7.32	6.48	5.98	5.11	4.56
0.350	32.89	29.04	25.49	22.21	19.27	17.45	15.19	13.53	12.33	10.87	9.88	9.06	7.96	7.28	6.46	5.97	5.11	4.57
0.375	32.82	28.32	24.74	21.61	18.59	16.85	14.73	13.15	12.02	10.58	9.68	8.77	7.81	7.17	6.38	5.67	5.07	4.55
0.400	32.60	28.08	24.41	21.31	18.39	16.66	14.57	13.04	11.93	10.50	9.59	8.72	7.78	7.14	6.37	5.67	5.07	4.55
0.425	32.38	27.80	24.14	21.00	18.15	16.38	14.39	12.89	11.79	10.38	9.50	8.64	7.72	7.07	6.32	5.64	5.05	4.54
0.450	32.03	27.43	23.57	20.53	17.84	16.04	14.09	12.65	11.58	10.21	9.36	8.52	7.61	6.99	6.25	5.57	5.01	4.50
0.475	31.24	27.10	22.89	19.73	17.18	15.44	13.55	12.20	11.20	9.87	9.06	8.26	7.40	6.82	6.14	5.47	4.94	4.46
0.500	29.78	25.44	20.58	17.38	14.83	13.30	11.52	10.43	9.41	8.41	7.71	7.06	6.38	5.78	5.40	4.91	4.53	4.19

Table 4. The denoising capacity interconnection of PSNR and the stable constant T_0 for LENA image

Fix	PNSR (dB)																	
cons.	5	10	15	20	25	30	35	40	45	50	55	60	65	70	75	80	85	90
0.025	25.34	25.82	24.23	23.44	22.50	24.58	20.21	19.06	17.53	15.85	13.87	10.72	8.43	7.53	6.05	6.09	6.18	5.69
0.050	30.43	28.84	27.68	25.97	24.00	22.84	**21.03**	**19.51**	**17.82**	**16.17**	14.15	11.24	9.22	8.16	6.19	6.13	6.20	5.69
0.075	29.33	29.55	28.76	26.95	**24.77**	**22.98**	20.98	19.45	17.68	16.07	**14.18**	**11.17**	9.70	8.55	6.87	6.43	6.31	5.96
0.100	36.48	29.45	28.68	**27.14**	24.76	22.58	20.50	18.97	17.15	15.67	13.92	11.71	**10.38**	8.90	7.28	6.39	**6.48**	5.15
0.125	38.57	27.77	**29.30**	26.66	23.77	21.82	19.65	18.22	16.24	15.03	13.05	11.61	10.28	**8.95**	7.54	6.87	6.36	**6.17**
0.150	40.02	**34.48**	28.13	22.96	22.49	20.71	18.73	17.14	15.36	14.04	12.66	11.06	9.93	8.57	7.47	6.76	6.30	6.09
0.175	**40.03**	33.18	27.54	25.09	21.49	19.54	17.60	15.89	14.35	13.13	11.81	10.39	9.36	8.12	**7.55**	6.77	6.23	5.95
0.200	38.62	31.35	26.67	23.81	20.40	18.44	16.68	15.19	13.74	12.63	11.31	10.18	9.04	8.00	7.29	6.61	6.06	5.83
0.225	36.57	29.97	25.48	22.76	19.56	17.91	16.20	14.80	13.42	12.37	11.21	9.94	9.01	7.98	7.28	6.71	6.22	5.82
0.250	34.26	28.16	24.12	21.59	18.74	17.17	15.68	14.42	12.99	12.10	11.03	9.90	9.10	7.99	7.35	7.01	6.20	5.97
0.275	32.00	26.60	22.84	20.51	14.99	16.74	14.97	13.80	12.62	11.32	10.73	9.66	9.03	8.08	7.07	6.95	6.16	6.08
0.300	30.15	25.39	21.75	19.52	17.57	16.05	14.45	13.20	12.04	11.23	10.22	9.43	8.34	8.12	7.05	7.01	6.05	5.79
0.325	28.82	24.31	20.79	18.63	16.80	15.94	13.90	12.68	11.61	10.84	9.88	9.03	8.40	8.07	7.22	**7.05**	6.27	6.07
0.350	27.60	23.23	19.92	17.89	16.05	14.68	13.32	12.18	11.16	10.39	9.52	8.78	8.24	7.92	7.16	6.76	6.33	6.08
0.375	26.60	22.17	19.09	17.11	15.34	14.05	12.73	11.71	10.74	9.98	9.23	8.52	8.07	7.59	7.09	6.74	6.40	6.09
0.400	25.65	21.37	18.49	16.55	14.92	13.69	12.45	11.47	10.51	9.80	9.09	8.43	8.00	7.53	7.06	6.71	6.39	6.09
0.425	24.93	20.72	17.90	16.09	14.57	13.39	12.22	11.29	10.37	9.68	.00	8.38	7.96	7.49	7.04	6.69	6.36	6.05
0.450	24.28	20.16	17.43	15.68	14.23	13.11	12.00	11.09	10.23	9.57	8.93	8.32	7.91	7.45	7.02	6.67	6.33	6.02
0.475	23.43	19.49	16.88	15.22	13.81	12.76	11.71	10.86	10.06	9.43	8.82	8.23	7.85	7.42	7.01	6.67	6.34	6.04
0.500	22.79	18.88	16.39	14.83	13.45	12.45	11.49	10.67	9.89	9.31	8.73	2.18	7.82	7.41	7.02	6.70	6.39	6.08

4.2. The experimental investigation of image denoising method found on DBAMF

This analyzed report focuses to examine the computational scrutiny of image denoising method found on DBAMF under SPN surrounding. In this examining of the DBAMF denoising capacity, four analyzed images, which are contained of Airplane, Pepper, Girl and Lena, are used to analyzed by initially adding synthesized SP noise for creating numerous distorted portraits. Later, all distorted portraits are repaired for obtaining the finest quality and best PSNR by executing the image denoising method found on DBAMF. From the above examining, the denoising methods by applying AMF [7, 25] and DBAMF produce the finest quality and best PSNR than other denoising methods for instant SMF and Gaussian filter. However, the DBAMF has marginally improved than AMF from that fact that the DBAMF is initially developed solely for random magnitude impulsive noise (RMIN) but the AMF is developed solely for SPN. From these computer examining of the denoising capacity in Table 5(a) for Lena and Pepper and Table 5(b) for Girl and Airplane, althrogh the DBAMF denoising method is originally desired for RVIN, the DBAMF denoising method can provide the fine results (the denoised images with high quality). From these inverstigation, the DBAMF method and adaptive median filter (AMF) can produce the denoised image with finer quality and high PSNR, which is confronted with the other denoised images, which is computed by standard median filter (SMF) and Gaussian Filter. Due to circumspection of sheet of paper, some

graphical results (of Lena image at 10% and 20%) of the denoised DBAMF method and other denoised methods are shown in Figure 4.

Table 5 (a). The analysis report of the denoising capacity of DBAMF under SPN surrounding

SPN			PNSR (dB)			
Operated images	Noise density	LR image	Noise suppressing technique			
			Median (3x3)	Mean (3x3)	AMF	DBA MF
Lena	D=0.05	18.7139	31.6421	22.4181	36.0907	40.0318
(256x256)	D=0.10	15.6564	30.7076	19.3812	35.3032	34.4817
	D=0.15	13.8274	29.2982	17.5385	33.7454	29.3024
	D=0.20	12.6389	27.6257	16.3208	32.1558	27.1381
	D=0.25	11.6783	25.4101	15.3526	29.8105	24.7729
	D=0.30	10.8971	23.6811	14.5829	27.9141	22.9755
	D=0.35	10.2240	20.8127	13.8785	25.6654	21.0287
	D=0.40	9.6481	19.0080	13.2479	23.7903	19.5071
	D=0.45	9.0745	16.8389	12.6598	21.5949	17.8200
	D=0.50	8.6553	15.4758	12.2146	20.5725	16.1734
	D=0.55	8.2118	13.8573	11.7609	19.4896	14.1775
	D=0.60	7.7813	12.3280	11.2939	18.1747	11.7120
	D=0.65	7.4884	11.3251	11.0012	17.7283	10.3838
	D=0.70	7.1697	10.2861	10.6509	17.1153	8.9514
	D=0.75	6.8497	9.1271	10.2599	16.5388	7.5456
	D=0.80	6.5846	8.3331	10.0057	16.4554	7.0520
	D=0.85	6.3241	7.5344	9.7338	16.4230	6.4819
	D=0.90	6.0604	6.8241	9.4356	16.5352	6.1742
Pepper	D=0.05	18.4752	32.2578	22.1408	37.1145	37.5975
(256x256)	D=0.10	15.3798	30.6116	19.0677	36.0391	32.8628
	D=0.15	13.5570	28.8470	17.2234	33.6095	28.5840
	D=0.20	12.3593	26.5888	15.9804	31.6485	25.9117
	D=0.25	11.3929	24.2073	14.9986	29.4205	23.6700
	D=0.30	10.6242	22.0663	14.1748	26.7650	21.7606
	D=0.35	9.9742	20.3774	13.5209	25.5249	20.3507
	D=0.40	9.3998	18.4321	12.9076	23.4995	18.4004
	D=0.45	8.8599	16.6168	12.3275	21.7177	17.0967
	D=0.50	8.3843	14.8506	11.8117	20.2203	15.3313
	D=0.55	7.9930	13.4655	11.3720	19.0894	13.5815
	D=0.60	7.6189	12.0128	10.9563	18.1116	11.9462
	D=0.65	7.2684	10.8920	10.5158	17.3657	10.3517
	D=0.70	6.9246	9.7704	10.2039	16.5923	8.9034
	D=0.75	6.6418	8.8751	9.8955	16.2338	7.8407
	D=0.80	6.3710	8.0166	9.252.	16.0896	7.0426
	D=0.85	6.1097	7.2402	9.2949	16.0498	6.5095
	D=0.90	5.8582	6.5767	9.0214	16.2932	6.2081

Table 5 (b). The analysis report of the denoising capacity of DBAMF under SPN surrounding

SPN			PNSR (dB)			
Operated images	Noise density	LR image	Noise suppressing technique			
			Median (3x3)	Mean (3x3)	AMF	DBA MF
Girl	D=0.05	16.4490	32.4867	20.0454	37.5895	39.2037
(256x256)	D=0.10	13.6890	31.5583	17.2530	36.9197	35.9413
	D=0.15	11.9287	27.6179	15.3515	34.818	32.0931
	D=0.20	10.6567	25.5153	13.9593	32.0437	29.3961
	D=0.25	9.5498	22.9614	12.7148	29.6074	26.069
	D=0.30	8.8677	20.7738	11.9599	27.6930	23.2608
	D=0.35	8.0984	18.4410	11.0501	34.9709	20.5962
	D=0.40	7.5798	1635146	10.4543	23.3736	18.4867
	D=0.45	7.0728	14.8145	9.8471	21.8119	16.9252
	D=0.50	6.5712	13.0319	9.2367	20.1712	15.1631
	D=0.55	6.2085	11.8226	8.7895	19.2184	13.6912
	D=0.60	5.8609	10.4981	8.3590	18.4518	12.2929
	D=0.65	5.4832	3.1396	7.8712	17.2740	10.9353
	D=0.70	5.1311	8.0463	7.4271	16.7334	9.5595
	D=0.75	4.8712	7.1994	7.0814	16.2921	8.703
	D=0.80	4.5674	6.2520	6.6881	16.2795	7.5002
	D=0.85	4.3054	5.4218	6.3340	16.5924	6.5222
	D=0.90	4.0573	4.7465	5.9986	16.7463	5.2931
Airplane	D=0.05	17.9498	31.4106	21.5802	36.6063	36.5023
(256x256)	D=0.10	14.8320	29.6532	18.4426	34.6311	31.5421
	D=0.15	13.1197	28.3176	16.6870	33.5561	29.9163
	D=0.20	11.8045	26.4356	15.3181	31.3844	26.2166
	D=0.25	10.9272	24.4147	14.3866	29.5029	25.0114
	D=0.30	10.0510	21.8862	13.4526	27.1347	22.1793
	D=0.35	9.4325	19.6835	12.7646	26.0118	20.5242
	D=0.40	8.8735	17.6412	12.1397	23.0147	18.5963
	D=0.45	8.3344	15.8686	11.5224	21.2768	17.0442
	D=0.50	7.8600	14.2697	11.0091	19.6201	15.4295
	D=0.55	7.4696	12.8823	10.5769	18.6408	13.9249
	D=0.60	7.0920	11.5290	10.1202	17.6586	12.3281
	D=0.65	6.7276	10.4080	9.7008	16.9400	10.9416
	D=0.70	6.4028	9.3041	9.3238	16.2514	9.8385
	D=0.75	6.1274	8.3797	9.0020	15.9223	8.6814
	D=0.80	5.8647	7.5835	8.6893	15.7428	7.9942
	D=0.85	5.5768	6.7043	8.3346	15.8098	6.9951
	D=0.90	5.3335	6.0278	8.0381	16.0834	6.3296

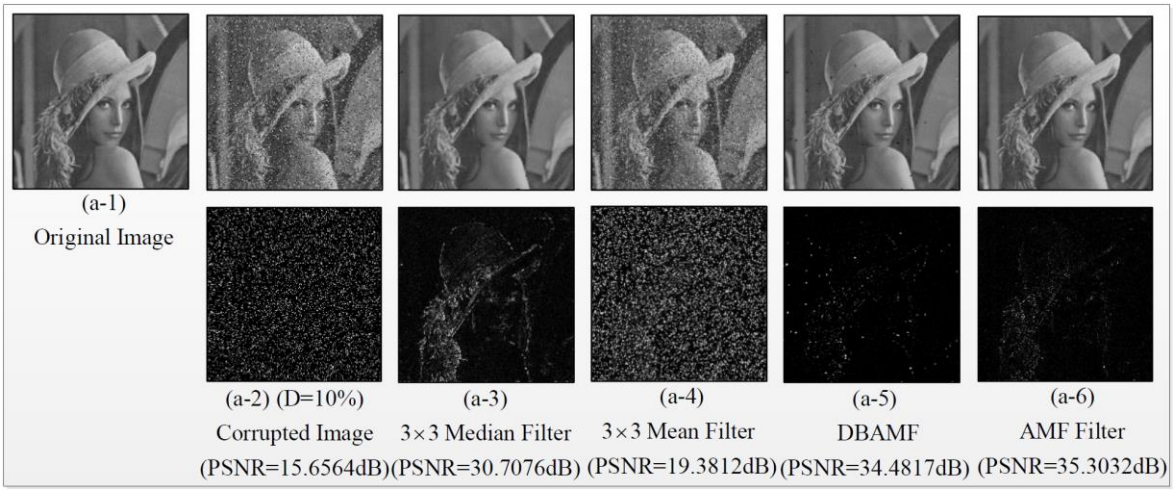

(a)

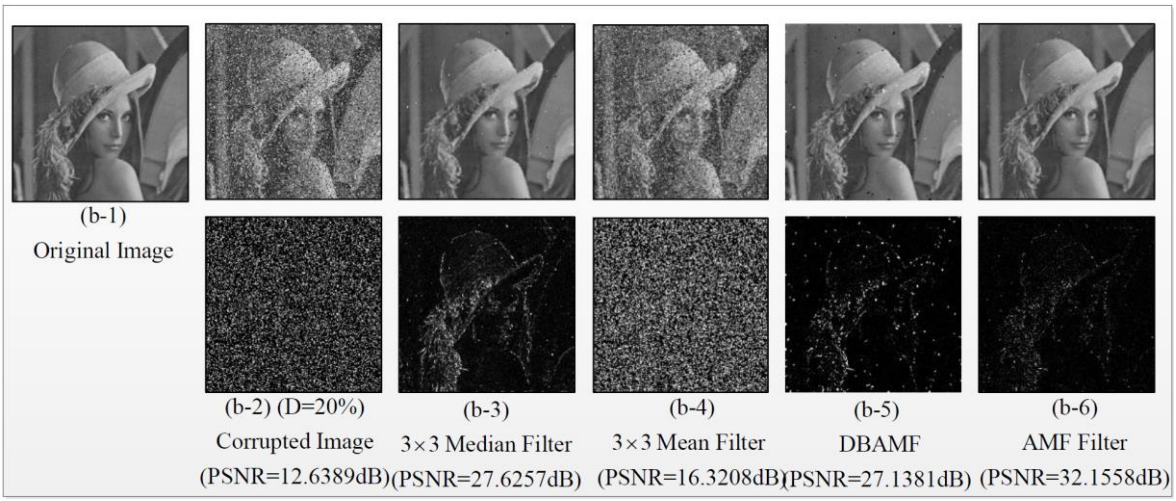

(b)

Figure 4. The analysis report of noise repairing method of the DBAMF

5. CONCLUSION

This analyzed report focuses to examine the similarity capacity of denoising method found on DBAMF for diverse SPN Surrounding. In order to examine the denoising capacity and its obstruction of the denoising method found on DBAMF, the four original digital images, comprised of Airplane, Pepper, Girl and Lena, are examined in these computational simulation for SPN surrounding by initially contaminating the SPN with diverse intensity. The first constribution of this report is the optimized stable constant, which is determined from computer simulation at SPN surrounding. Later, the second contribution of this report is the overall capacity of denoising method found on DBAMF, confronted with the other denoised images (SMF and gaussian filter and adaptive median filter (AMF)) under the SPN with diverse intensity.

ACKNOWLEDGEMENTS

The research project was funded by Assumption University.

REFERENCES

[1] A. Awad, "Removal of fixed-valued impulse noise based on probability of existence of the image pixel," *International Journal of Electrical & Computer Engineering,* vol. 8, no. 4, pp. 2106-2114, 2018.

[2] H. Hwang and R. A. Haddad, "Adaptive median filters new algorithms and results," *IEEE Transactions of Image Processing,* vol. 4, pp. 4, pp. 499-502, 1994.

[3] Kornkamol Thakulsukanant and Vorapoj Patanavijit, "Simulation evaluation of noise suppressing technique based on decision based adaptive median filter for salt & pepper noise," *16th International Conference on Electrical Engineering/Electronics, Computer, Telecommunications and Information Technology,* pp. 585-588, 2019.

[4] K. Arun Sai, K. Ravi, "An efficient filtering technique for denoising colour images," *International Journal of Electrical and Computer Engineering (IJECE),* vol. 8, no. 5, pp. 3604-3608, 2018.

[5] R. H. Chan, C-W Ho and M. Nikilova, "Salt & pepper noise removal by median-type noise detectors and detail-preserving regularization," *IEEE Transactions of Image Processing,* vol. 14, no. 10, pp. 1479-1485, 2005.

[6] V. Patanavijit, "The bilateral denoising performance influence of window," *Spatial and Radiometric Variance,* 2015.

[7] V. Patanavijit, "Performance analysis of denoising algorithm based on adaptive median filter under unsystematic intensity impulse and salt & pepper noise," *International Electrical Engineering Congress,* pp. 1-4, 2018.

[8] W. K. Pratt, "Median filtering," *Tech. Rep., Image Proc. Inst.,* Univ. Southern California, Los Angeles, 1975.

[9] Yiqiu Dong, Raymond H. Chan, and Shufang Xu, "A detection statistic for random-valued impulse noise," *IEEE Transactions on Image Processing,* vol. 16, no. 4. pp. 1112-1120, 2007

[10] Om Prakash Verma and Nitin Sharma, "Intensity preserving cast removal in color images using particle swarm optimization," *International Journal of Electrical & Computer Engineering,* vol. 7, no. 5, pp. 2581-2595, 2017.

[11] Madina Hamiane and Fatema Saeed, "SVM classification of MRI brain images for computer-assisted diagnosis, *International Journal of Electrical and Computer Engineering,* vol. 7, no. 5, pp. 2555-2564, 2017.

[12] A. S. M. Shafi, et.al., "Decomposition of color wavelet with higher order statistical texture and convolutional neural network features set based classification of colorectal polyps from video endoscopy," *International Journal of Electrical and Computer Engineering*, vol. 10, no. 3, pp. 2986-2996, 2020.

[13] S. Bagchi, et.al, "Image processing and machine learning techniques used in computer-aided detection system for mammogram screening-A review," *International Journal of Electrical and Computer Engineering*, vol. 10, no. 3, pp. 2336-2348, 2020.

[14] César G. Pachón-Suescún, Carlos J. Enciso-Aragón, Robinson Jiménez-Moreno, "Robotic navigation algorithm with machine vision," *International Journal of Electrical and Computer Engineering*, vol. 10, no. 2, pp. 1308-1316, 2020.

[15] D. Kesrarat, et.al, "A novel elementary spatial expanding scheme form on sisr method with modifying geman & mcclure function," *TELKOMNIKA Telecommunication, Computing, Electronics and Control,* vol. 17, no.5, 2019.

[16] V. Patanavijit, "Denoising performance analysis of adaptive decision based inverse distance weighted interpolation (DBIDWI) algorithm for salt and pepper noise," *Indonesian Journal of Electrical Engineering and Computer Science,* vol. 15, no. 2, pp. 804-813, 2019.

[17] V. Kishorebabu1, et.al., "An adaptive decision based interpolation scheme for the removal of high density salt and pepper noise in images," *EURASIP Journal on Image and Video Processing,* vol. 2017, no. 1, 2017.

[18] V. Patanavijit, et.al, "The statistical analysis of random-valued impulse noise detection techniques based on the local image characteristic: ROAD, ROLD and RORD," *Indonesian Journal of Electrical Engineering and Computer Science*, vol. 15, no. 1, pp.749-803, 2019.

[19] Y. Dong, et.al, "A detection statistic for random-valued impulse noise," *IEEE Transactions on Image Processing,* vol. 16, no. 4, pp. 1112-1120, 2007.

[20] H. Yu, et.al, "An efficient procedure for removing random-valued impulse noise in images," *IEEE Signal Processing Letters,* vol. 15, pp. 922-925, 2008.

[21] V. Jayaraj and D. Ebenezer, "A New Switching-BasedMedian Filtering Scheme and Algorithm for Removal of High-Density Salt and Pepper Noise in Images," *EURASIP JASP*, 2010.

[22] Ali S. Awad, "Standard Deviation for Obtaining the Optimal Direction in the Removal of Impulse Noise," *IEEE Signal Letters,* 2011.

[23] V. Patanavijit and K. Thakulsukanant, "Simulated Evaluation of New Switching Based Median Filter for Suppressing SPN and RVIN," *Indonesian Journal of Electrical Engineering and Computer Science*, Vol. 15, No. 2, Aug. 2019.

[24] R. C. Gonzalez and R. E. Woods, "Digital Image Processing," *Prentice Hall*, 2nd edition, NJ, USA, 2002.

[25] V. R. Vijaykumar and P. Jothibasu, "Decision Based Adatpvive Median Filter to Remove Blotches, Scratches, Streaks, Stripes and Impulse Noise in Images," *2010 IEEE International Conference on Image Processing*, Hong Kong, pp. 117-120, September 2010.